The effect of MQL on tool wear progression in low-frequency vibration-assisted drilling of CFRP/Ti6Al4V stack material

Ramy Hussein (Husser2@mcmaster.ca)
McMaster University https://orcid.org/0000-0001-8216-1251
Ahmad Sadek
Aerospace Manufacturing, National Research Council Canada
Mohamed Elbestawi (elbestaw@mcmaster.ca)
McMaster University
Helmi Attia
McGill University; Advanced Material Removal Technology, National Research Council Canada

Research Article

Keywords: Vibration-assisted drilling, Low-frequency vibration-assisted drill, CFRP/ Ti6Al4V, Stacked material, Minimum quantity lubricant, Surface integrity, Delamination, Burr formation, Tool wear

Posted Date: February 15th, 2021

DOI: https://doi.org/10.21203/rs.3.rs-168821/v1

Abstract

In this paper, the tool wear mechanism in low-frequency vibration-assisted drilling (LF-VAD) of carbon fiber reinforced polymer (CFRP)/Ti6Al4V stacks has been proposed using variably machining parameters. Based on the kinematics analysis, the effect of vibration amplitude on the chip formation, uncut chip thickness, chip radian, and axial velocity was presented. Subsequently, the effect of LF-VAD on the cutting temperature, tool wear, delamination, and geometrical accuracy was presented for different vibration amplitude. The LF-VAD with the utilization of minimum quantity lubricant (MQL) resulted in a successful drilling process of 50 holes, with a 63 % reduction of the cutting temperature. For the rake face, LF-VAD reduced the adhered height of Ti6Al4V by 80 % at low cutting speed and reduced the crater depth by 33 % at the high cutting speed. On the other hand, LF-VAD reduced the flank wear land by 53 %. Furthermore, LF-VAD showed a significant enhancement on the CFRP delamination, geometrical accuracy, and burr formation.

1 Introduction

The rapid advancements in the new generation of aircraft, explains the growing usage of lightweight materials in the hybrid structure design [1]. This structure commonly consists of carbon fiber-reinforced polymer (CFRP) and the Ti6Al4V titanium alloy in different coupling forms such as CFRP/Ti6Al4V, CFRP/Ti6Al4V/CFRP, and Ti6Al4V/CFRP/ Ti6Al4V [2, 3]. Compared to the usage of uni-material structure, the hybrid design showed a superior physical and mechanical properties such as high strength-to-weight ratio, low coefficient of thermal expansion, corrosion/erosion, and fatigue resistance [4, 5]. The mechanical fastening using rivets and bolts is commonly used during the assembly process of these materials. Consequently, the single drilling process of the CFRP/Ti6Al4V stack materials has been identified as an effective method to achieve high precision assembly and productivity.

A swift tool wear progress was identified as one of the major challenges during the practical one-shot drilling process of CFRP/Ti6Al4V stack materials [6, 7]. This tool wear progression can be described by two main mechanisms. Abrasive wear of the hard carbon fiber particles [8–11], and adhesion wear mechanism during the drilling process of Ti6Al4V. The machining process of Ti6Al4V resulted in a significant increases on the cutting tool temperature due to the low thermal conductivity, and the continuous chip morphology of Ti6Al4V [11, 12]. The high cutting temperature has a severe effect on the cutting tool condition, particularly during the drilling process where the poor evacuation mechanism located. Consequently, this process has a high tendency of chip accumulation and the tool-chip welding takes place [11, 13]. Furthermore, by increasing the cutting tool temperature, the tool material suffers from the low hardness properties. Hence, the on-shot drilling process of CFRP/Ti6Al4V will shows a severe abrasion wear mechanism from the CF particles. Thus, reducing the cutting temperature and segmenting the titanium chips have been emphasized by several studies.

Conventional drilling (CD) parameter optimization [7, 14, 15], pick-up drilling [16], orbital drilling [17, 18], and vibration-assisted drilling (VAD) [19, 20], are of the main strategies that have been investigated to

reduce the cutting temperature and change the titanium chips morphology. Based on machining productivity, the VAD is the most promising machining method for stacked materials. In VAD, an axial tool oscillation is superimposed on to the normal tool feed direction, to generate an interrupted drilling process [21, 22]. The interrupted cutting resulted in substitute the continuous Ti6Al4V chip morphology by segmented chips with a controllable geometry [23, 24]. This achievement resulted in a better chips evacuation efficiency with a preferable cyclic cutting/cooling duty [23]. Thus, lower cutting temperature, better geometric accuracy, high surface quality, and compressive residual stresses can be induced [19, 20, 23, 25, 26].

Despite the promising results of LF-VAD in terms of tool durability, the presented investigations failed to discuss two main factors; the machining productivity and the associated effect of tool wear progression on the hole quality. The investigated range of cutting speed was limited by 20 m/min [26, 27], without any clarification of the associated hole quality that represents the critical criteria for the aerospace industry. In a previous study [25], the effect of LF-VAD on tool wear and the associated hole quality was presented using cutting speeds up to 56.52 m/min which is three-folds the illustrated range, using a recommended vibration amplitude [11]. The study was conducted using a dry coolant condition that resulted in reduce the cutting tool temperature by up to 40 %. However, the dry coolant condition showed an unsuccessful drilling process of 50 holes that attributed to the observation of the tool-chip welding process.

The utilization of LF-VAD with forced air resulted in decrease the cutting temperature by up to 51.3 %, enhance the chips evacuation efficiency, and reduces the tool-chip welding probability [27]. Despite the slight thermal load reduction compared to the dry coolant, the presented study was limited to 20 m/min cutting speed which had a negative impact on the machining productivity. Furthermore, the author did not show the effect of forced air medium on the machined surface quality. Hence, the usage of a proper coolant medium could resulted in a substantial enhancement on the cutting tool life and machining performance.

Minimum quantity lubricant (MQL) is a technology used to approach the tool/workpiece interface with a minimum amount of coolant medium to achieve the economic and environmental profits [28]. In terms of cutting temperature, tool life, and machining performance, the utilization of MQL showed a significant enhancement during the CD and LF-VAD process of CFRP/Ti6Al4V, as presented in [28, 29]. The combination effect of LF-VAD and MQL coolant showed 42 % reduction on the cutting temperature with a long tool life. This achievement could be the first step toward a high process stability for the automated drilling operation. However, a comprehensive study using a high cutting speed range and presenting the associated effect on the machining performance is highly recommended.

The current study presents the effect of LF-VAD under MQL coolant medium on the tool wear progression and the associated hole quality. The tool analysis covers the tool flank surface, rake surface, and the chisel edge. This analysis was correlated to the kinematics of VAD for a better understanding. Furthermore, the study presents a clear comparison between the effect of LF-VAD in dry and MQL conditions, for the same machining parameters.

2 Experimental Setup

All the experiments were carried out on a five-axis CNC machining center (Makino A 88), with the MITIS tool holder. This tool holder has a fixed 2.5 oscillation/rev modulation frequency with a variable amplitude selection range (0.01 to 0.48 mm). The cutting tool temperature was monitored at the exit surface using the FLIR SC8000 HD series infrared camera. As recommended for the aerospace manufacturer, A 6 mm uncoated tungsten carbide (WC) twist drill was utilized during the conducted test matrix. The tool has a 118° point angle with coolant through for MQL supply. The workpiece material has CFRP/Ti6Al4V stack sequence with a 120 mm side length. The CFRP has a total thickness of 5.8 mm, while the Ti6Al4V plate has a 6.75 mm thickness. Based on the previous experimental investigation [11, 25],Table 1 presents the selected machining parameters, tool, and workpiece materials. The test matrix consisted of two-level of cutting speeds (2000 and 3000 rpm), three levels of vibration amplitudes (0.1, 0.16, and 0.25 mm), and fixed feed rate of 0.075 mm/rev. The selected test matrix parameters are targeting to overcome the previously published machining issues, as presented in [11]. The applied minimum quantity lubricant (MQL) has a 5 % concentration of the MECAGREEN 550 with a 100 bar pressure.

Table 1: Specification of machining parameters, tool, and workpiece.

Machining Parameters		
Cutting Speed, N	rpm	2,000 and 3,000
Feed rate, f	mm/rev	0.075
Amplitude, A_m	mm	0.1, 0.16, and 0.25
Cooling medium		MQL
Cutting Tool		
Material		Tungsten Carbide
Diameter		6 mm
Point angle		118°
Helix angle		20°
Manufacturer		YG-1
Workpiece material specification		
CFRP		- 5.8 ± 0.02 mm of 42 × L-930(GT700) woven plies with the configuration $[[0,90]_{21}]$s, and flame retardant modified epoxy prepreg. - Decomposition temperature is 320°C.
Titanium alloy		Ti6Al4V grade 5
Stacking sequence		CFRP 5.8 ± 0.02 mm/Ti6Al4V 6.75 ± 0.02 mm

The tool wear analysis was based on a continuous drilling process of 50 drilled holes. The Winslow engineering tool analyzer model 560 was used for the rake and flank surface examination. To investigate and identify the tool wear mechanisms, the scanning electron microscopy (SEM) and energy-dispersive X-ray spectroscopy (EDS) were used. The rake face surface topography was inspected using the Alicona instrument. The CFRP delamination was analyzed using the Keyence digital microscope VHX-6000 series. The Mitutoyo Coordinate Measuring Machine (CMM) was used to measure the drilled hole diameter error based on the average of ten points on two surfaces of each material.

3 Kinematics Of Vad

Discarding the non-cutting machining process under the chisel edge through the axial tool oscillation for the vibration-assisted drilling, it showed a recommended enhancement during the drilling process of CFRP/Ti6Al4V, as presented in [25]. Based on the instantaneous cutting edge trajectory as described in equation (1-3), the effect of vibration amplitude and cutting speed on the axial tool velocity has been investigated.

$$Z_1 = \frac{\gamma}{360^\circ} * f + A * \sin(\gamma * F) \quad (1)$$

$$Z_2 = \frac{(\gamma - 180^\circ)}{360^\circ} * f + A * \sin[(\gamma - 180) * F] \quad (2)$$

The dynamic uncut chip thickness could be expressed as:

$$t_o = \begin{cases} Z(\gamma) - \max(Z_k(\gamma)) & , Z(\gamma) > \max(Z_k(\gamma)) \\ 0 & , otherwise \end{cases} \quad (3)$$

Where max ($Z_k(\gamma)$) represents the maximum height of the preceding rotation.

During the drilling process of LF-VAD, increasing the vibration amplitude showed an obvious change on the chip formation, as shown in Figure 1. Based on equation (3), the calculated uncut chip thickness was 0.15 mm for all vibration amplitudes, which is double the programmed feed. However, increasing the A_m results in reducing the chip radian by 30 %. The chip radian reduced from 65° at A_m= 0.1 mm to 45° at A_m= 0.25 mm. This reduction has a direct impact on the cutting tool temperature and the tool wear mechanism during the drilling process of Ti6Al4V layer.

Figure 2 presents the axial tool velocity at different vibration amplitude and cutting speed. The vibrational amplitude was identified as the dominant effective parameter controlling the axial tool velocity followed by the cutting speed. Consequently, the increase of A_m would result in a proper cooling environment, low exit delamination factor, and higher evacuation efficiency. However, increasing the axial tool velocity could result in a severe tool-workpiece impact that resulted in a chisel edge fracture. Hence, chisel edge inspection is highly recommended to identify the vibration amplitude threshold at the onset of chisel fracture.

4 Results And Discussion

4.1 Cutting temperature

The effect of tool wear progression on the cutting tool temperature was measured at the exit surface of the Ti6Al4V layer for different cutting speeds and vibration amplitudes, as shown in Figure 3. For all machining conditions, LF-VAD showed a significant reduction in the cutting temperature compared to the CD. This reduction percentage was increased from 55% for A_m= 0.1 mm to 65% for A_m= 0.25 mm at *N*= 2000 rpm, and from 45% for A_m= 0.1 mm to 68% for A_m= 0.25 mm at *N*= 3000 rpm. This enhancement was due to the positive effect of higher vibration amplitude that reduced the duty cycle and increased the

cooling cycle [23]. As a consequence, the MQL was more efficient at higher A_m to achieve lower cutting temperatures.

Compared to the CD at *N*= 2000 rpm, the analysis of the results showed that the cutting tool temperature under LF-VAD was reduced by 40 % for dry coolant condition [11], and 65 % for MQL coolant condition, respectively, as shown in Figure 4. For high cutting speed (*N*= 3000 rpm), tool-chip welding has been confirmed as the main issue that resulted in stopping the drilling process at the second hole for CD, and hole number 20 for LF-VAD with A_m= 0.25 mm, as reported in [11]. The use of MQL resulted in a successful machining process of 50 drilled holes without any observation of the tool-chip welding process. This achievement was traced back to the significant reduction of the cutting tool temperature, lower tool-chip friction, and the higher chip evacuation efficiency as a secondary effect of MQL.

4.2 Tool wear progression and mechanism

4.2.1. Flank face

Figure 5 presents the measured flank wear land for different vibration amplitudes and cutting speeds. Compared to CD, LF-VAD resulted in a lower flank wear land for all machining conditions. For the low cutting speed *N*= 2000 rpm, the tool life was enhanced by increasing A_m. Compared to CD at drilled hole number 50 (flank wear = 135 µm), the flank wear land was reduced by 37 %, 45 %, and 53 % for A_m= 0.1 mm, A_m= 0.16 mm, and A_m= 0.25 mm, respectively, as shown in Figure 5(a). The reason for these reductions is the lower cutting temperature at higher vibration amplitude, as described in section 4.2. Compared to dry machining condition, the MQL did not show a considerable effect on the flank wear land for CD and LF-VAD at A_m= 0.25 mm. For both machining condition, the flank wear land was reduced by 8 µm at drilled hole number 50. This ineffective behavior of MQL at these machining conditions was assigned to the continuous tool-workpiece contact at CD, and excessive coolant time for A_m= 0.25 mm. On the other hand, by up to 50% reduction on the flank wear land, the MQL is more efficient at A_m= 0.16 mm. This effect could be discussed by the relatively low cooling interval, and consequently the temperature gradient at MQL is highly recommended. Moreover, the smaller air gap width that works on increases the MQL efficiency, as discussed in [30].

For the high cutting speed *N*= 3000 rpm, increasing the vibration amplitude does not affect the flank wear land for the first 30 drilled hole, and a reduction of 30 % was measured for all A_m. However, by increasing the drilled holes number, the LF-VAD with the lowest vibration amplitude becomes favorable, as shown in Figure 5(b). This effect could be the result of the higher transformation rate from the steady to severe wear regions for LF-VAD as an effect of high A_m due to the relatively high thrust force, as reported in [23]. Unlike the low cutting speed, MQL showed a significant enhancement at *N*= 3000 rpm. The MQL resulted in a successful drilling process of 50 holes with acceptable flank wear land, according to ISO 3685 (≤ 300 µm) [31].

Furthermore, the relatively low cutting temperature and the intermitted cutting process of LF-VAD showed a significant limitation on chemical wear compared to the CD [27]. Based on the tool flank surface examination, the colored area and Built-up edge were prominent in CD, while the LF-VAD showed a discolored surface with a limited Built-up edge, as shown in Figure 6.

4.2.2. Chisel edge

The scanning electron microscopy (SEM) examination of the tool chisel edge revealed such a clear difference between CD and LF-VAD process, as shown in Figure 7 and Figure 8. For CD, there is obvious evidence of Ti adhesion to the chisel edge for both cutting speeds (Figure 7(a) and Figure 8(a)). This observation was due to the relatively higher cutting temperature in CD compared to LF-VAD, as discussed in section 4.2 due to the poor chip evacuation mechanism [25]. On the other hand, the chisel edge fracture was identified as a dominant mechanism for LF-VAD, as shown in (Figure 7(b,c) and Figure 8(b,c)). This observation supports the negative effect of the high axial tool velocity which resulted in a severe tool-workpiece impact mechanism, as described in section 3. Contrary to [26], the chisel edge suffers a severe fracture rather than Ti adhesion due to the negative clearance angle. This difference could be attributed to the utilization of higher A_m range (0.1 to 0.25 mm) compared to only 0.06 mm. Furthermore, the observation of an extensive chisel edge fracture at A_m= 0.25 mm Figure 7 (c), clarify the significant thrust force increase at hole number 45 for *N*= 2000 rpm, as described in section 4.1.

The thermal impact was identified as one of the critical drawbacks during the intermitted machining process [32, 33]. Inducing the cutting tool material to a frequent temperature variation resulted in a thermal crack formation [33-35]. Consequently, increase the temperature gradient through the utilization of a coolant medium during the LF-VAD process could increase the probability of thermal cracks initiation or tool fracture. Compared to dry machining condition [11], the MQL resulted in the observation of chisel edge fracture for both cutting speeds. This observation could be attributed to the relatively high thermal gradient during the uses of MQL. Based on the flank surface and chisel edge analysis, dry coolant condition is highly recommended for low cutting speed condition, while MQL is required for the higher cutting speed.

4.2.3. Rake face

Surface topography was examined to identify the main tool wear mechanism for each machining condition, as shown in Figure 9 and Figure 10. Figure 9 shows the examined rake face surface for different A_m after the drilling process of an identical number of 50 holes at *N*= 2000 rpm. Adhesion and abrasion wear mechanisms were observed for all machining conditions. However, the adhesion wear mechanism had the dominant effect, specially for the CD condition. This effect was attributed to the relatively higher cutting temperature for the CD. The high chemical affinity toward most of the industrially used drill bits material highlights adhesion as a dominant wear mechanism during the drilling process of Ti materials [4, 11, 26, 36, 37]. This process resulted in a built-up edge (BUE) formation, that leads to tool fracture or chipping and consequently, poor hole quality and short tool life will be observed. Based on the

surface topography analysis, the greatest height of defects was 400 µm for CD, 90 µm for A_m= 0.1 mm, 75 µm for A_m= 0.16 mm, and 160 µm for A_m= 0.25 mm. The LF-VAD resulted in a significant reduction of the adhered particles height by up to 80 % at A_m= 0.16 mm. However, increasing the vibration amplitude to A_m= 0.25 mm showed a relatively lower reduction percentage of 60%. This effect could be due to the higher effect of MQL turbulence or the probability of collision between the small radian chips at A_m= 0.25 mm [23, 24], and the borehole wall. In addition, by SEM examination of the drill bit rake face used for CD, a considerable amount of carbon fiber was found adhered to the BUE as shown in Figure 10 and confirmed by the EDS analysis in Table 2. This adhesion could be due to the tool-borehole wall interaction during the tool retraction that could have a negative effect on the CFRP geometric accuracy and surface roughness.

Figure 11shows the effect of different vibration amplitudes at *N*= 3000 rpm on the rake face after the drilling process of identical 50 holes. The crater wear mechanism was identified as the dominant wear for all machining conditions. This change in the tool wear mechanism was the result of the relatively higher cutting temperature at *N*= 3000 rpm. The maximum crater depth was measured and plotted, as shown Figure 12. Compared to the CD, the LF-VAD resulted in a lower crater depth with up to 33 % reduction at A_m= 0.25 mm, as shown in Figure 12. The lower crater depth for LF-VAD at high A_m was attributed to the lower cutting temperature, as discussed in section 4.2. Moreover, increasing the A_m resulted in a significant reduction in the tool-chip contact time, as presented in [23]. This reduction has a positive impact on restricting the adhesion wear on the tool rake surface.

Table 2: The EDS analysis for the selected points, as shown in Figure 10(b).

	C	Al	Ti	V	Co	W	Total
Spectrum 1	43.42	3.86	49.57	3.15	0	0	100.00
Spectrum 2	97.43	0.65	0.47	0.40	0.25	0.80	100.00

4.3 Effect of tool wear on the exit delamination.

Based on the CFRP exit surface examination, the drilling process of CFRP/Ti6Al4V commonly results in discoloration ring and damaged area [38]. The discoloration ring was caused due to the cutting temperature at the CFRP/Ti6Al4V interface surface. While the Ti6Al4V chips evacuation mechanism resulted in severe damage of the borehole wall. Table 3 presents the effect of tool wear on the exit delamination for different vibration amplitudes and cutting speeds. The delamination factor (φ_d) was identified based on the following equation [21, 39]:

$$\emptyset_d = \frac{D_{actual} - D_{nominal}}{D_{nominal}}$$

where D_{actual} is the diameter of a circle including the discoloration ring and all damaged area, while $D_{nominal}$ represents the nominal hole diameter.

For all machining conditions, the measured φ_d was acceptable, as defined by aerospace manufacturers ($\varphi_d \leq 0.5$) [21]. However, free exit delamination was successfully achieved by using LF-VAD with A_m= 0.1 mm and 0.16 mm, as shown in Figure 13. This observation was attributed to the lower cutting temperature and the proper chip evacuation efficiency. The slight increase of φ_d for A_m= 0.25 mm could be due to the negative effect of dynamic tool movement at this amplitude.

Table 3: The effect of tool wear on the exit delamination for different vibration amplitudes and cutting speeds.

Cutting speed (rpm)	Vibration amplitude (mm)	Drilled hole number				
		0 - 10	10 - 20	20 - 30	30 - 40	40 - 50
N= 2000	Conventional	0.1 – 0.2				
	A_m= 0.1	Free				
	A_m= 0.16					
	A_m= 0.25	Free	0.05 – 0.1			
N= 3000	Conventional	0.05 – 0.1		0.1 – 0.2		0.2 – 0.3
	A_m= 0.1	Free				
	A_m= 0.16					
	A_m= 0.25	0.05 – 0.1				

4.4 Effect of tool wear on the geometrical accuracy.

Based on the aerospace manufacturers' recommendations, the acceptable hole size error was identified from – 0.7 % to 0.4 % [21]. For both cutting speeds, CD exceeds the acceptable CFRP hole size, as shown in Figure 14(a,b). This unacceptable hole size was a result of the destructive effect of Ti6Al4V chips during evacuation. On the contrary, the LF-VAD with A_m= 0.16 mm and 0.25 mm, resulted in an acceptable accuracy for *N*= 2000 rpm and the first 25 drilled hole at *N*= 3000 rpm. The unacceptable hole accuracy after drilled hole number 25 could be reverted to the negative effect of flank wear land progression. In addition, the LF-VAD with A_m= 0.1 mm, resulted in a relatively higher chip radian [13], that could reduce the chips evacuation efficiency thus increasing the negative damage effect on the CFRP wall. On the other hand, both machining processes resulted in an acceptable Ti6Al4V hole accuracy for all drilled holes at different cutting speeds, as shown in Figure 14(c,d). However, the LF-VAD with A_m= 0.16 mm and 0.25 mm, showed the lowest geometric deviation for both cutting speeds.

4.5 Burr height

Thermal load and thrust force are of the main machining characteristics that control the material burr formation at the exit surface during the drilling process. For CD, the burr height increased from 0.4 mm at the first drilled hole, to 0.7 mm at drilled hole number 50, as shown in Figure 15(a,b). This increase was attributed to the higher cutting temperature, as discussed in section 4.2. For LF-VAD at the first drilled hole, the burr height was 1.2 mm and 1.36 mm, for A_m= 0.1 mm and A_m= 0.25 mm, respectively. The

higher burr compared to CD was attributed to the higher thrust force, as discussed in section 4.1. Conversely, increasing the drilled hole number with LF-VAD showed a positive effect, compared to CD. The measured burr height at drilled hole number 50 was reduced to 1.04 mm and 0.57 mm for A_m= 0.1 mm and A_m= 0.25 mm, respectively as shown in Figure 15(c,d). This reduction could be attributed to the chisel edge fracture as observed and discussed in section 4.3. This fracture increases the tool-workpiece contact area under the chisel edge that resulted in reducing the applied stresses magnitude on the machined material, and consequently a lower driving force for burr formation. Furthermore, maintaining a low cutting temperature for A_m= 0.25 mm resulted in a further burr height reduction compared to A_m= 0.1 mm, as shown in Figure 15 (d,f).

4.6 MQL vs Dry coolant condition

Based on the exit delamination analysis during dry machining condition [11] and the MQL coolant medium, Figure 16 presents the effect of each coolant condition on the observed machining process at N= 2000 rpm. For the CD, MQL showed a significant enhancement on the exit delamination factor and Ti hole accuracy. However, the geometrical accuracy of CFRP has an unacceptable range for both machining conditions. On the other hand, MQL is only useful for LF-VAD at *N*= 3000 rpm, while at low *N*= 2000 rpm both machining conditions have the same exit delamination factor.

Conclusions

This paper presents the effect of LF-VAD at relatively severe machining conditions (high cutting speeds and feed rates). The kinematics of VAD were used to predict and identify the impact of different machining conditions on the uncut chip thickness, cutting time, and the axial tool velocity. The utilization of Minimum quantity lubricant (MQL) showed a significant enhancement of the drilling performance compared to the dry drilling process as presented previously [11]. The following points highlight the main conclusion:

- The kinematics analysis of VAD showed a clear reduction of the chip radian and cutting time by increasing the vibration amplitude. However, this increase could raise the probability of chisel edge fracture due to the high axial velocity.
- LF-VAD resulted in a significant reduction of the cutting temperature by up to 63 % at high vibration amplitude.
- From the tool examination, the chisel edge was identified as the weakest point for LF-VAD. while for CD, the outer corner of the tool was the most vulnerable area for catastrophic failure due to the crater wear of the rake face at high cutting speed, or process termination due to excessive flank wear land at low cutting speed.
- The utilization of LF-VAD showed a reduction of 53 % and 30 % of the flank wear land for *N*= 2000 rpm, and *N*= 3000 rpm, respectively.

- The LF-VAD resulted in a reduction of 80 % of the maximum BUE height at N = 2000 rpm, while the crater depth was reduced by 33 % at N = 3000 rpm.
- The LF-VAD at A_m = 0.16 was recommended for a high machining performance at both cutting speeds.

Acronyms

VAD	Vibration assisted drilling
LF-VAD	Low frequency-vibration assisted drilling
CD	Conventional drilling
BUE	Built-up edge
MQL	Minimum quantity lubricant

Notations

N Cutting speed [rpm]

f Feed rate [mm/rev]

A_m Modulation amplitude [mm]

F Frequency [oscillation/rev]

W_f Modulation frequency [oscillation/rev]

Declarations

Acknowledgment This study was performed using the facilities of the Canadian National Research Council (CNRC), Aerospace Manufacturing Group. The use of their facilities, equipment and the technical support is greatly appreciated.

Authors' contributions: Ramy Hussein: investigation, methodology, conceptualization, and writing. Mohamed Elbestawi: review and editing, supervision. Ahmad Sadek: conceptualization, and resources. Helmi Attia: conceptualization, and resources.

Compliance with ethical standards

Ethical approval: Not applicable

Consent to participate: Not applicable

Consent to publish: Authors grant the publisher the sole and exclusive license of the full copyright.

Competing interests: The authors declare they have no competing interests

Funding: The research received no external funding

Data availability: The datasets generated during and/or analysed during the current study are currently not publicly available due to their use in an ongoing research but are available from the corresponding author on reasonable request.

References

[1] E. Brinksmeier and R. Janssen, "Drilling of Multi-Layer Composite Materials consisting of Carbon Fiber Reinforced Plastics (CFRP), Titanium and Aluminum Alloys," *CIRP Annals - Manufacturing Technology,* vol. 51, pp. 87-90, 2002/01/01/ 2002.

[2] J. Xu, A. Mkaddem, and M. El Mansori, "Recent advances in drilling hybrid FRP/Ti composite: a state-of-the-art review," *Composite Structures,* vol. 135, pp. 316-338, 2016.

[3] K.-H. Park, A. Beal, P. Kwon, and J. Lantrip, "A comparative study of carbide tools in drilling of CFRP and CFRP-Ti stacks," *Journal of Manufacturing Science and Engineering,* vol. 136, p. 014501, 2014.

[4] K.-H. Park, A. Beal, P. Kwon, and J. Lantrip, "Tool wear in drilling of composite/titanium stacks using carbide and polycrystalline diamond tools," *Wear,* vol. 271, pp. 2826-2835, 2011.

[5] J. Xu and M. El Mansori, "Wear characteristics of polycrystalline diamond tools in orthogonal cutting of CFRP/Ti stacks," *Wear,* vol. 376, pp. 91-106, 2017.

[6] I. Shyha, S. L. Soo, D. Aspinwall, S. Bradley, R. Perry, P. Harden*, et al.*, "Hole quality assessment following drilling of metallic-composite stacks," *International Journal of Machine Tools and Manufacture,* vol. 51, pp. 569-578, 2011.

[7] D. Kim and M. Ramulu, "Study on the drilling of titanium/graphite hybrid composites," *Journal of Engineering Materials and Technology,* vol. 129, pp. 390-396, 2007.

[8] S. Malhotra, "Some studies on drilling of fibrous composites," *Journal of Materials Processing Technology,* vol. 24, pp. 291-300, 1990.

[9] S. Lin and I. Chen, "Drilling carbon fiber-reinforced composite material at high speed," *Wear,* vol. 194, pp. 156-162, 1996.

[10] S. Rawat and H. Attia, "Wear mechanisms and tool life management of WC–Co drills during dry high speed drilling of woven carbon fibre composites," *Wear,* vol. 267, pp. 1022-1030, 2009.

[11] R. Hussein, A. Sadek, M. A. Elbestawi, and M. H. Attia, "An Investigation into Tool Wear and Hole Quality during Low-Frequency Vibration-Assisted Drilling of CFRP/Ti6Al4V Stack," *Journal of Manufacturing and Materials Processing,* vol. 3, p. 63, 2019.

[12] A. Poutord, F. Rossi, G. Poulachon, R. M'Saoubi, and G. Abrivard, "Local approach of wear in drilling Ti6Al4V/CFRP for stack modelling," *Procedia CIRP,* vol. 8, pp. 316-321, 2013.

[13] R. Hussein, A. Sadek, M. A. Elbestawi, and M. H. Attia, "Surface and microstructure characterization of low-frequency vibration-assisted drilling of Ti6Al4V," *The International Journal of Advanced Manufacturing Technology,* vol. 103, pp. 1443-1457, July 01 2019.

[14] D. Kim, C. Sturtevant, and M. Ramulu, "Usage of PCD tool in drilling of titanium/graphite hybrid composite laminate," *International Journal of Machining and Machinability of Materials,* vol. 13, pp. 276-288, 2013.

[15] O. Isbilir and E. Ghassemieh, "Comparative study of tool life and hole quality in drilling of CFRP/titanium stack using coated carbide drill," *Machining Science and Technology,* vol. 17, pp. 380-409, 2013.

[16] R. A. Weiss, *Portable air feed peck drilling of graphite composite, titanium and other materials in dissimilar combinations*: Society of Manufacturing Engineers, 1989.

[17] B. Denkena, D. Boehnke, and J. Dege, "Helical milling of CFRP–titanium layer compounds," *CIRP Journal of manufacturing Science and Technology,* vol. 1, pp. 64-69, 2008.

[18] H. Wang, X. Qin, H. Li, and Y. Tan, "A comparative study on helical milling of CFRP/Ti stacks and its individual layers," *The International Journal of Advanced Manufacturing Technology,* vol. 86, pp. 1973-1983, 2016.

[19] O. Pecat and E. Brinksmeier, "Low damage drilling of CFRP/titanium compound materials for fastening," *Procedia CIRP,* vol. 13, pp. 1-7, 2014.

[20] J. Lonfier and C. De Castelbajac, "A Comparison between Regular and Vibration-Assisted Drilling in CFRP/Ti6Al4V Stack," *SAE International Journal of Materials and Manufacturing,* vol. 8, pp. 18-26, 2015.

[21] A. Sadek, "Vibration Assisted Drilling of Multidirectional Fiber Reinforced Polymer Laminates," Ph.D. Thesis, McGill University Libraries, 2014.

[22] A. Sadek, M. Meshreki, and M. Attia, "Effect of Tool Kinematics on the Drilling Forces and Temperature in Low Frequency High Amplitude Vibration Assisted Drilling," in *ASME 2014 International Mechanical Engineering Congress and Exposition*, 2014, pp. V02AT02A035-V02AT02A035.

[23] R. Hussein, A. Sadek, M. A. Elbestawi, and M. H. Attia, "Surface and microstructure characterization of low-frequency vibration-assisted drilling of Ti6Al4V," *The International Journal of Advanced*

Manufacturing Technology, vol. 103, pp. 1443-1457, April 05 2019.

[24] O. Pecat and I. Meyer, "Low frequency vibration assisted drilling of aluminium alloys," in *Advanced Materials Research*, 2013, pp. 131-138.

[25] R. Hussein, A. Sadek, M. A. Elbestawi, and M. Attia, "Low-frequency vibration-assisted drilling of hybrid CFRP/Ti6Al4V stacked material," *International Journal of Advanced Manufacturing Technology,* vol. 98, pp. 2801-2817, Oct 2018.

[26] H. Yang, Y. Chen, J. Xu, M. Ladonne, J. Lonfier, and Y. Fu, "Tool wear mechanism in low-frequency vibration–assisted drilling of CFRP/Ti stacks and its individual layer," *The International Journal of Advanced Manufacturing Technology,* pp. 1-13, 2019.

[27] C. Li, J. Xu, M. Chen, Q. An, M. El Mansori, and F. Ren, "Tool wear processes in low frequency vibration assisted drilling of CFRP/Ti6Al4V stacks with forced air-cooling," *Wear,* vol. 426, pp. 1616-1623, 2019.

[28] M. Senthilkumar, A. Prabukarthi, and V. Krishnaraj, "Machining of CFRP/Ti6Al4V stacks under minimal quantity lubricating condition," *Journal of Mechanical Science and Technology,* vol. 32, pp. 3787-3796, 2018.

[29] O. Pecat and E. Brinksmeier, "Tool wear analyses in low frequency vibration assisted drilling of CFRP/Ti6Al4V stack material," *Procedia CIRP,* vol. 14, pp. 142-147, 2014.

[30] A. Sadek, M. Attia, M. Meshreki, and B. Shi, "Characterization and optimization of vibration-assisted drilling of fibre reinforced epoxy laminates," *CIRP Annals-Manufacturing Technology,* vol. 62, pp. 91-94, 2013.

[31] I. Standard, "3685," *Tool-life Testing with Single Point Turning Tools,* 1993.

[32] S. Kim, D. Lee, M. Kang, and J. Kim, "Evaluation of machinability by cutting environments in high-speed milling of difficult-to-cut materials," *Journal of materials processing technology,* vol. 111, pp. 256-260, 2001.

[33] Y. Su, N. He, L. Li, and X. Li, "An experimental investigation of effects of cooling/lubrication conditions on tool wear in high-speed end milling of Ti-6Al-4V," *Wear,* vol. 261, pp. 760-766, 2006.

[34] J. Vieira, A. Machado, and E. Ezugwu, "Performance of cutting fluids during face milling of steels," *Journal of Materials Processing Technology,* vol. 116, pp. 244-251, 2001.

[35] S. Yuan, L. Yan, W. Liu, and Q. Liu, "Effects of cooling air temperature on cryogenic machining of Ti–6Al–4V alloy," *Journal of Materials Processing Technology,* vol. 211, pp. 356-362, 2011.

[36] P. Zhang, N. Churi, Z. J. Pei, and C. Treadwell, "Mechanical drilling processes for titanium alloys: a literature review," *Machining Science and Technology,* vol. 12, pp. 417-444, 2008.

[37] S. Sharif and E. A. Rahim, "Performance of coated- and uncoated-carbide tools when drilling titanium alloy—Ti–6Al4V," *Journal of Materials Processing Technology,* vol. 185, pp. 72-76, 4/30/ 2007.

[38] M. Ramulu, T. Branson, and D. Kim, "A study on the drilling of composite and titanium stacks," *Composite Structures,* vol. 54, pp. 67-77, 10// 2001.

[39] R. Hussein, A. Sadek, M. A. Elbestawi, and M. H. Attia, "Chip Morphology and Delamination Characterization for Vibration-Assisted Drilling of Carbon Fiber-Reinforced Polymer," *Journal of Manufacturing and Materials Processing,* vol. 3, p. 23, 2019.

Figures

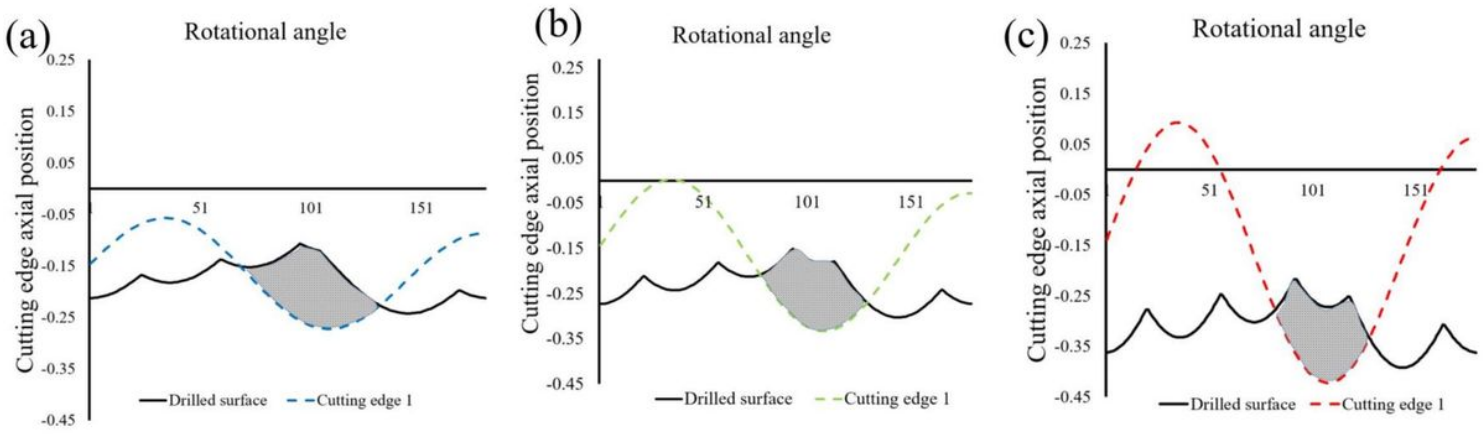

Figure 1

Effect of vibration amplitude on the uncut chip formation at (a) Am= 0.1 mm, (b) Am= 0.16 mm, and (c) Am= 0.25 mm.

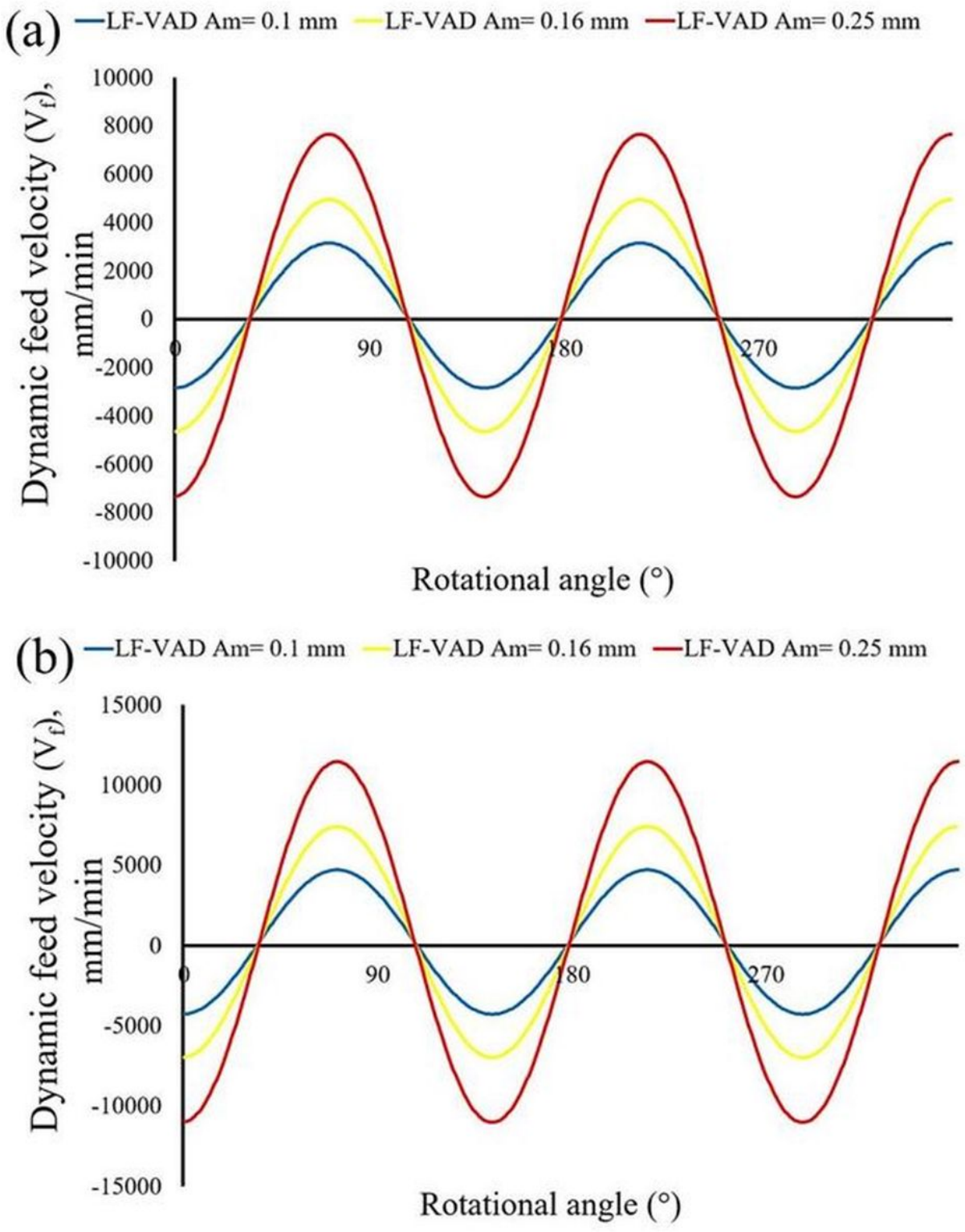

Figure 2

Effect of vibration amplitude (Am) on the axial tool velocity at different cutting speed (a) N= 2000 rpm (b) N= 3000 rpm.

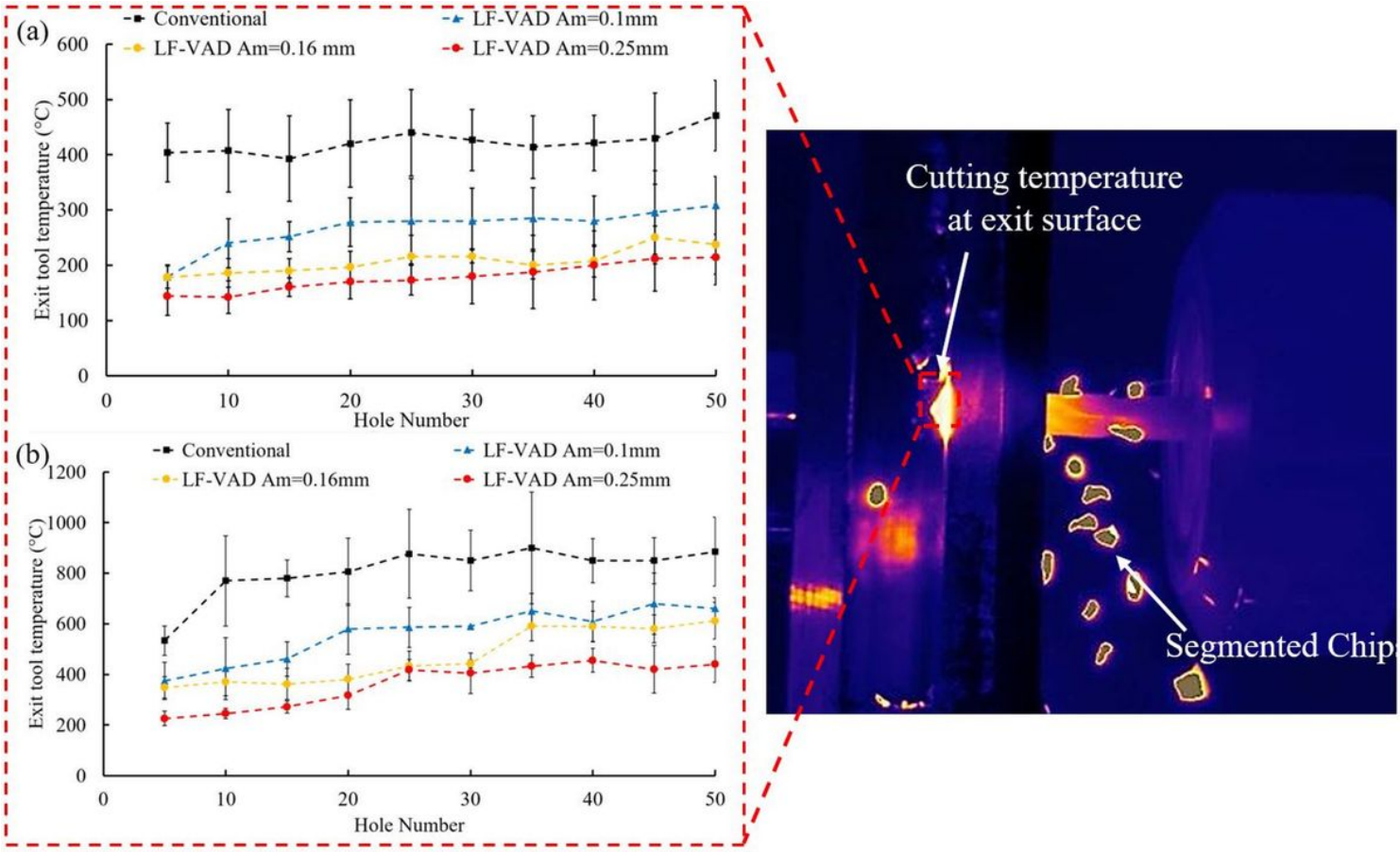

Figure 3

Effect of the tool wear progress on the tool cutting temperature at the exit surface for (a) N= 2000 rpm, and (b) N= 3000 rpm.

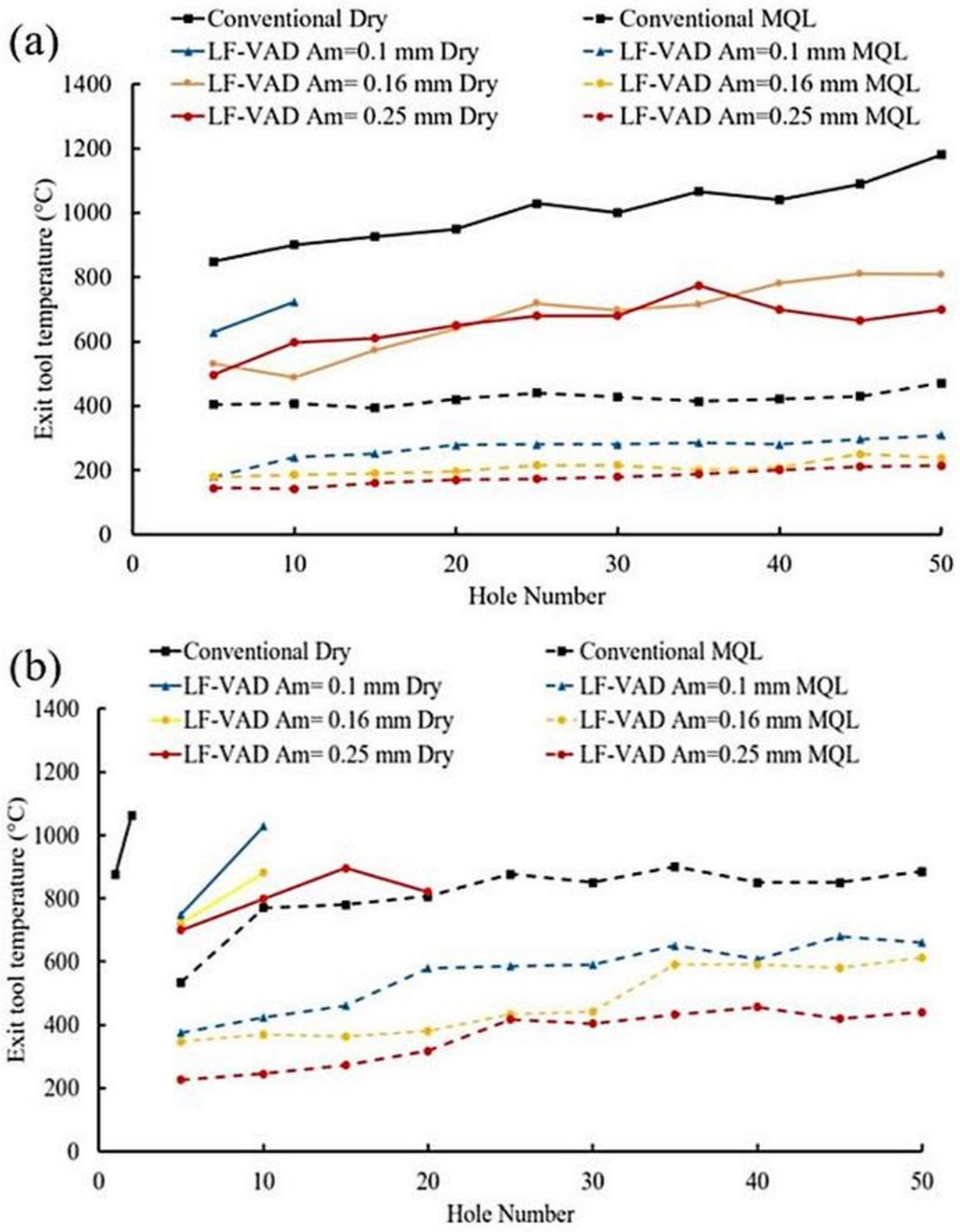

Figure 4

Effect of coolant medium on the cutting temperature for (a) N= 2000 rpm (b) N= 3000 rpm.

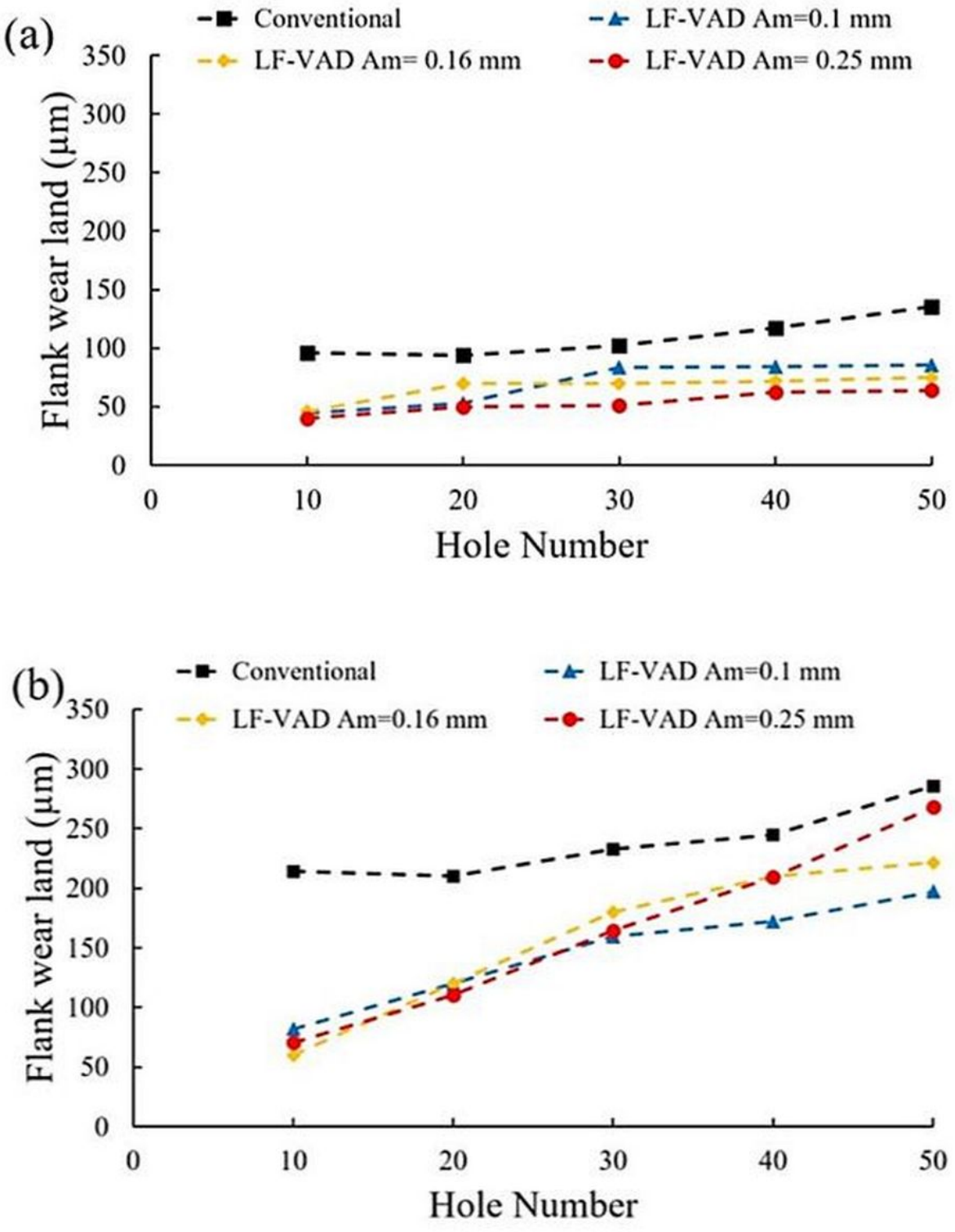

Figure 5

Effect of vibration amplitude on the tool flank wear land for different cutting speeds 2000 rpm (b) N= 3000 rpm.

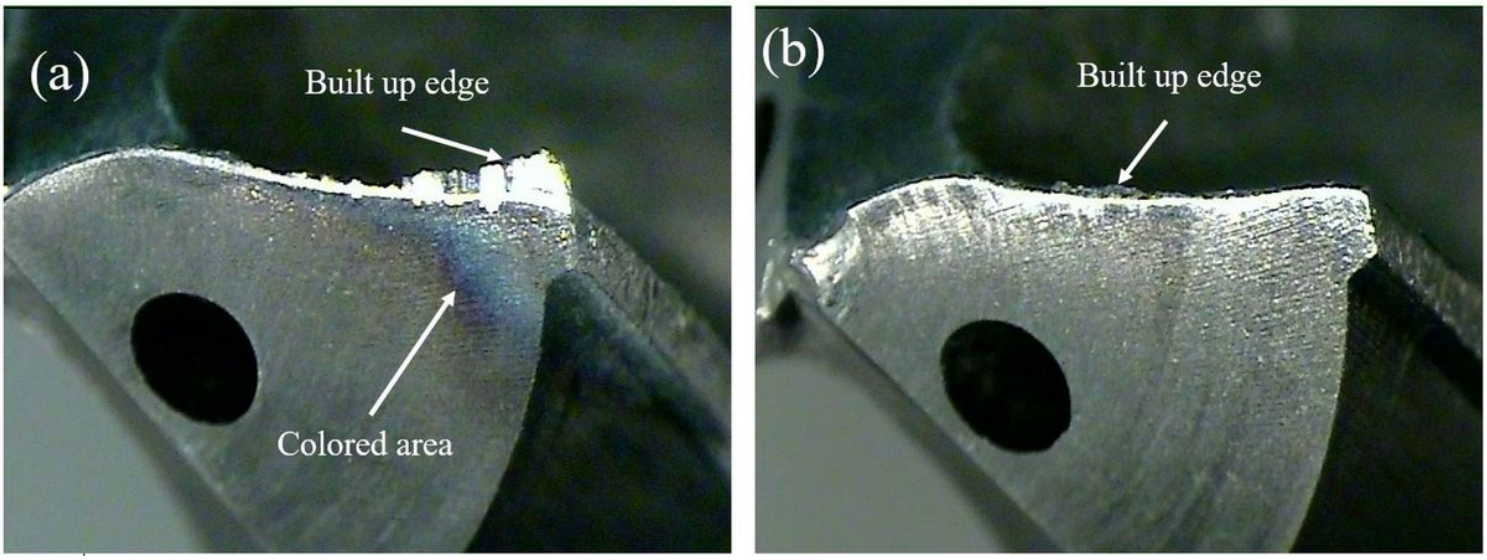

Figure 6

Effect of LF-VAD on the chemical wear and built-up edge formation for (a) conventional drill (b) Am= 0.16 mm.

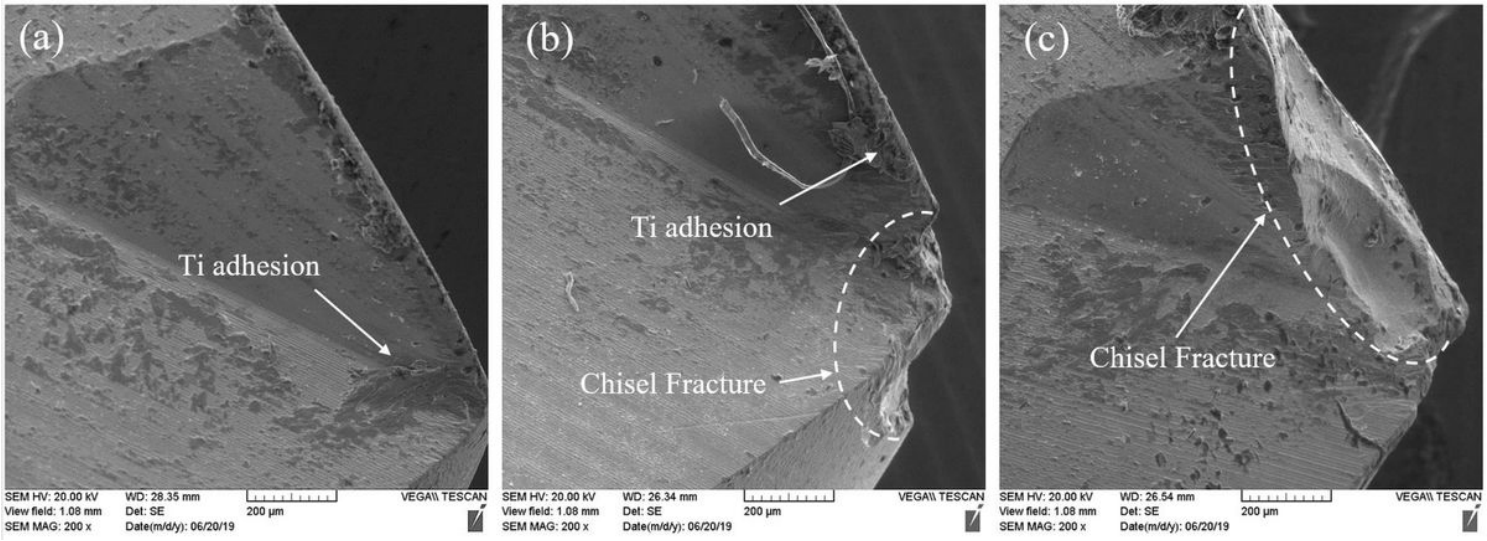

Figure 7

Effect of vibration amplitude on the tool chisel edge at N= 2000 rpm for (a) conventional, (b) Am= 0.1 mm, (c) Am= 0.25 mm.

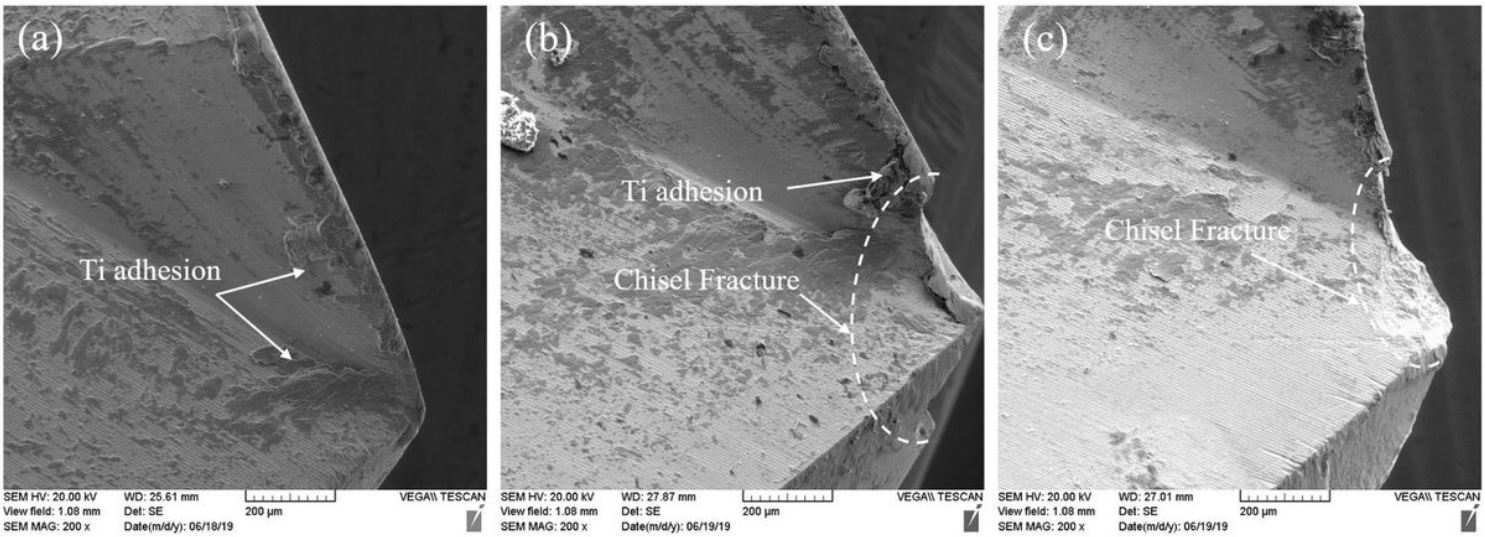

Figure 8

Effect of vibration amplitude on the tool chisel edge at N= 3000 rpm for (a) conventional, (b) Am= 0.1 mm, (c) Am= 0.25 mm.

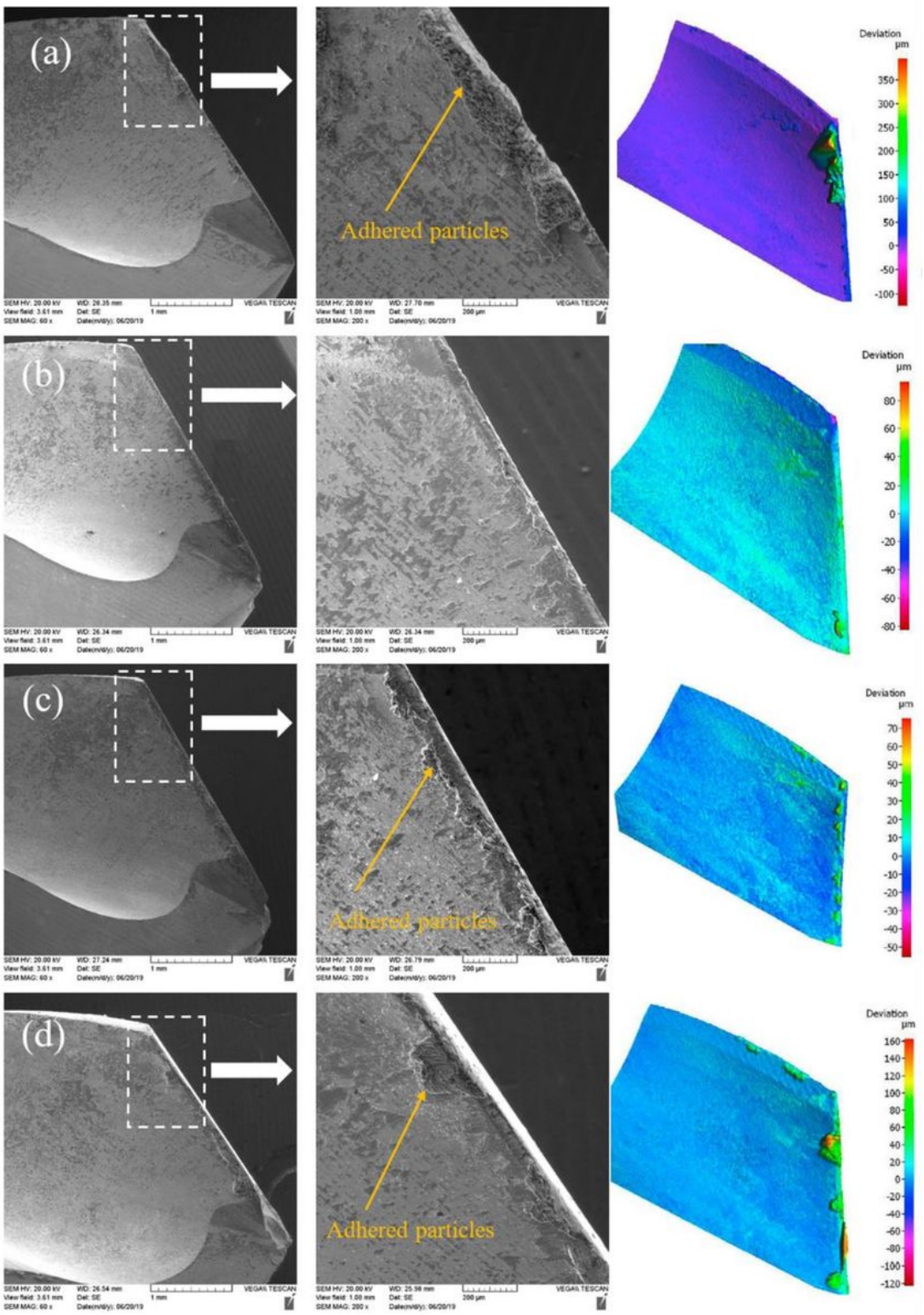

Figure 9

The SEM examination and surface topography analysis of the tool rake face at N= 2000 rpm for different vibration amplitude (a) Conventional, (b) Am= 0.1 mm, (c) Am= 0.16 mm, and (d) Am= 0.25 mm.

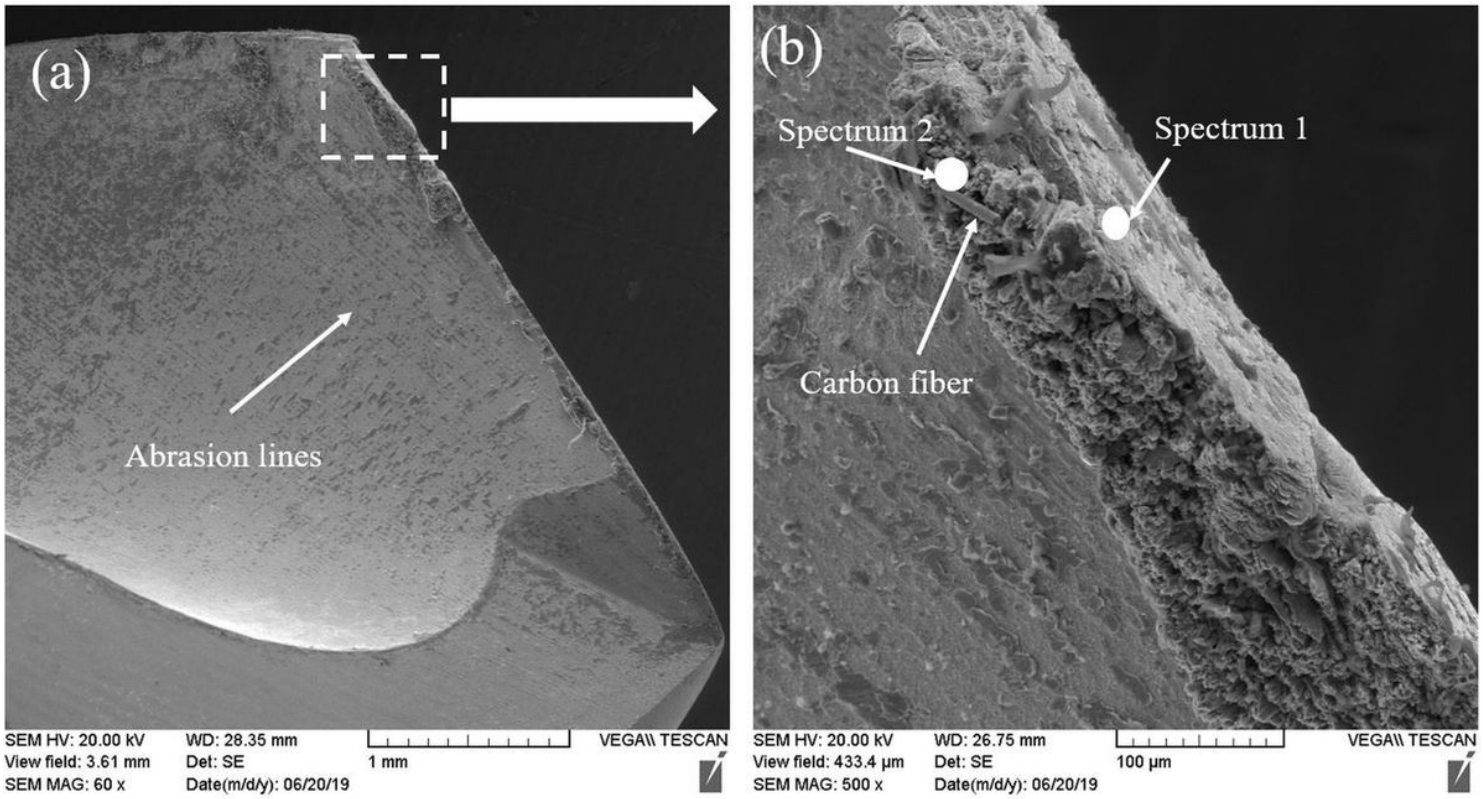

Figure 10

The conventional drill effect on the rake face after drilled hole number 50.

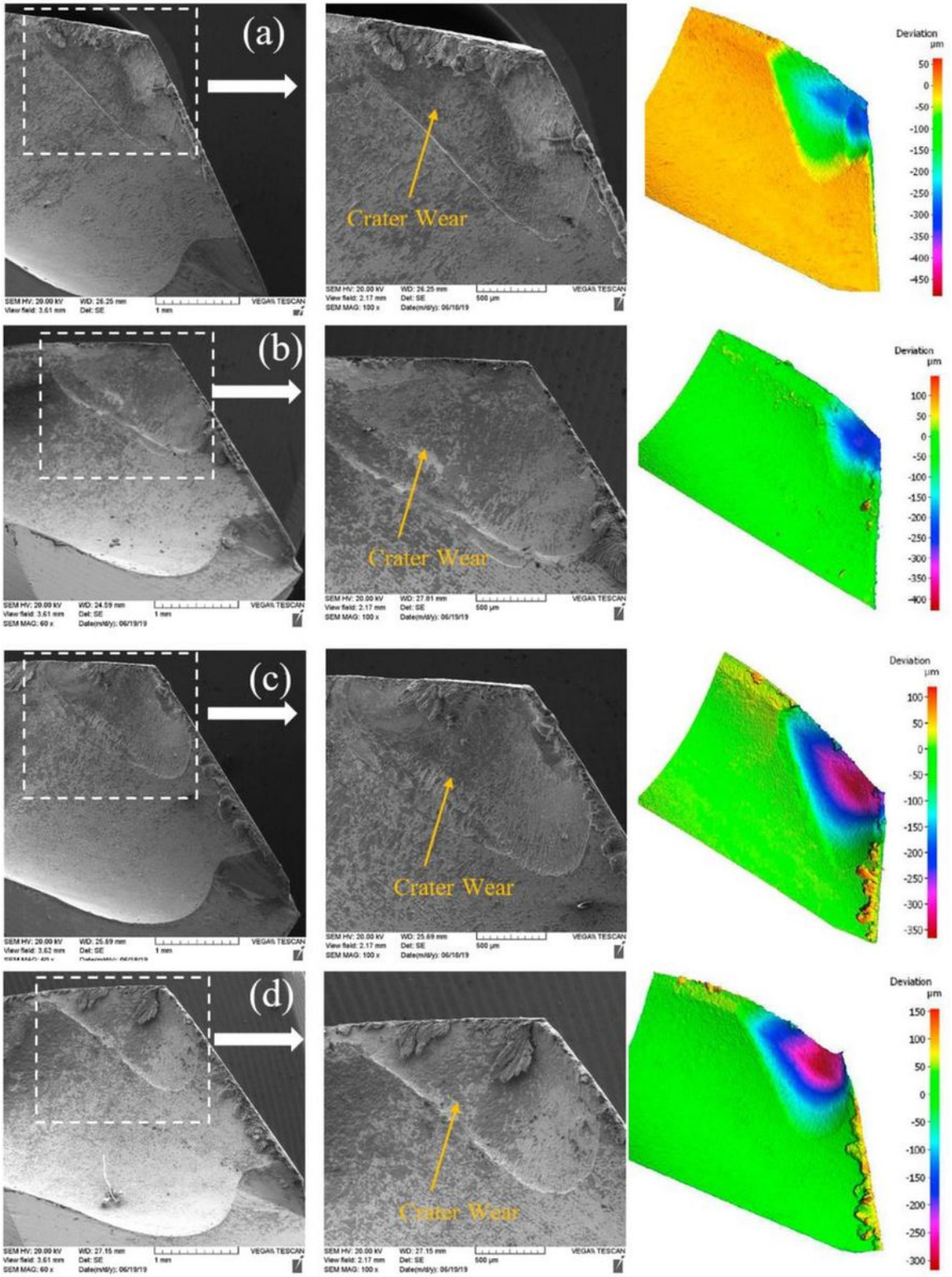

Figure 11

The SEM examination and surface topography analysis of the tool rake face at N= 3000 rpm for different vibration amplitude (a) Conventional, (b) Am= 0.1 mm, (c) Am= 0.16 mm, and (d) Am= 0.25 mm.

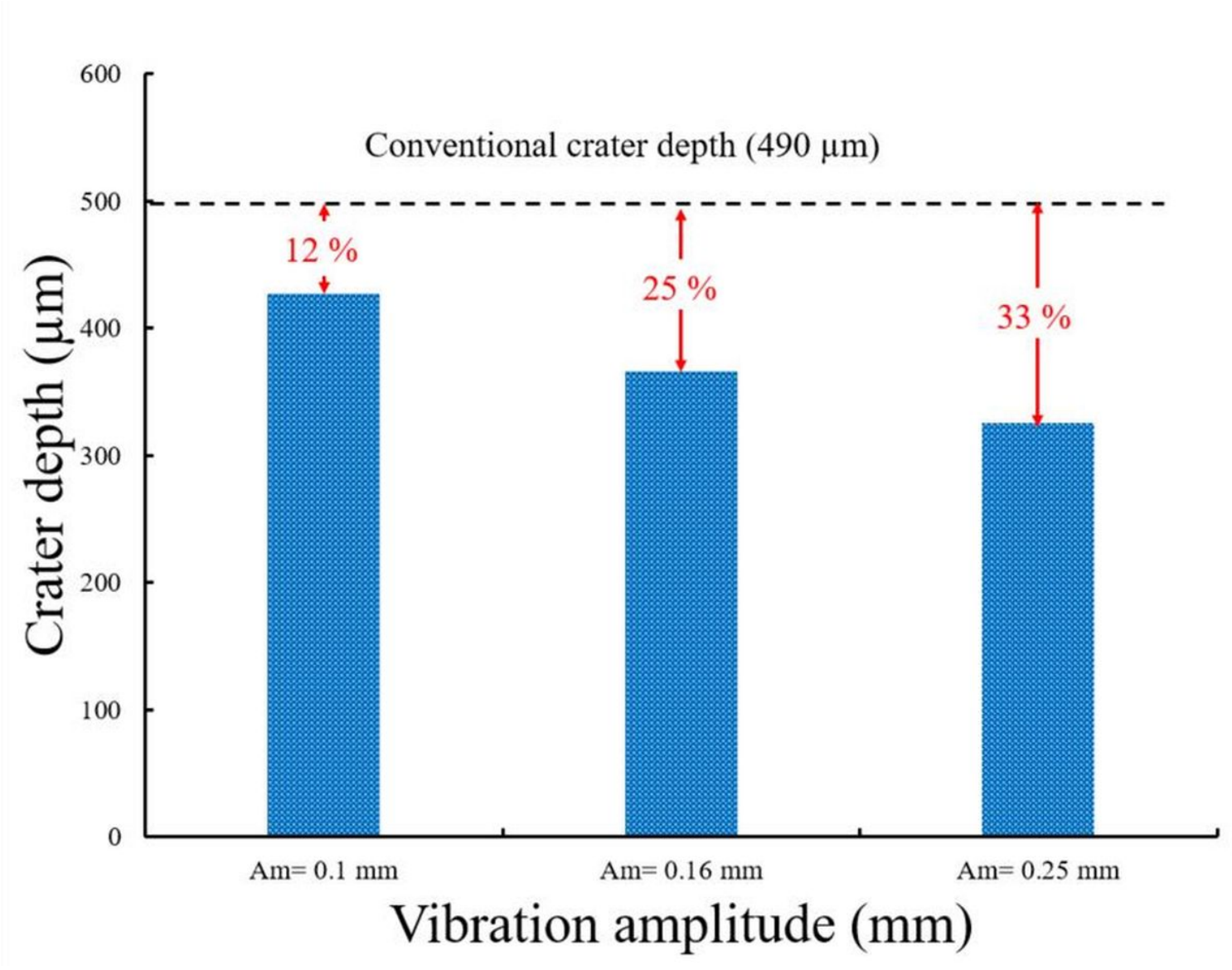

Figure 12

The measured crater depth at different vibration amplitude for N= 3000 rpm.

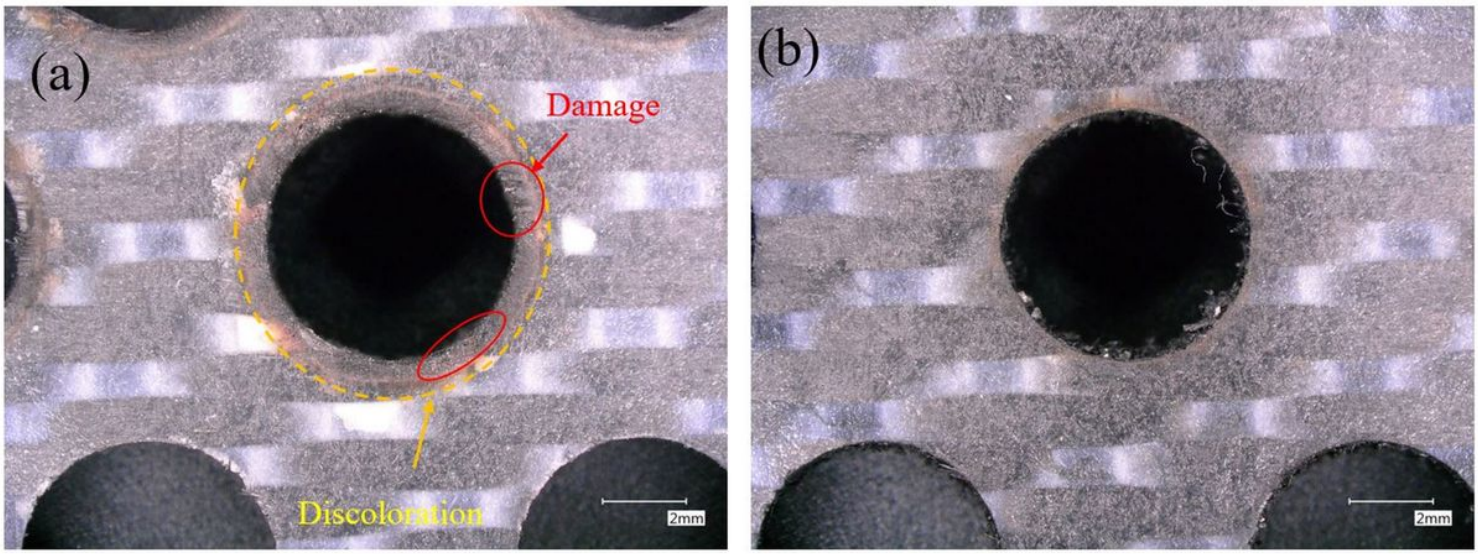

Figure 13

The effect of LF-VAD on the exit delamination for N= 3000 rpm (a) conventional (b) Am= 0.16 mm.

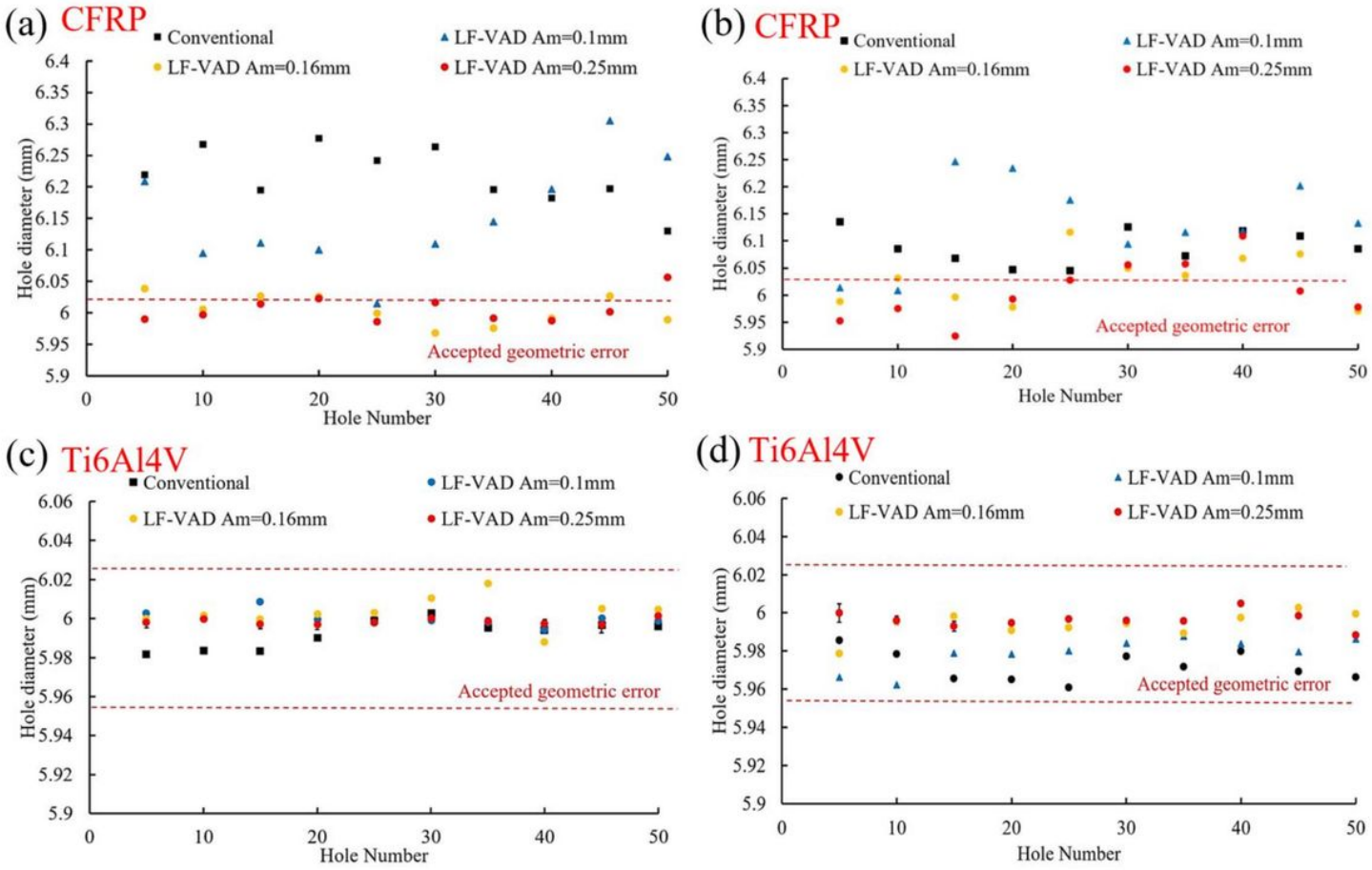

Figure 14

Effect of vibration amplitude on the CFRP and Ti6Al4V hole accuracy at different cutting speeds (a,c) N= 2000 rpm, (b,d) N= 3000 rpm

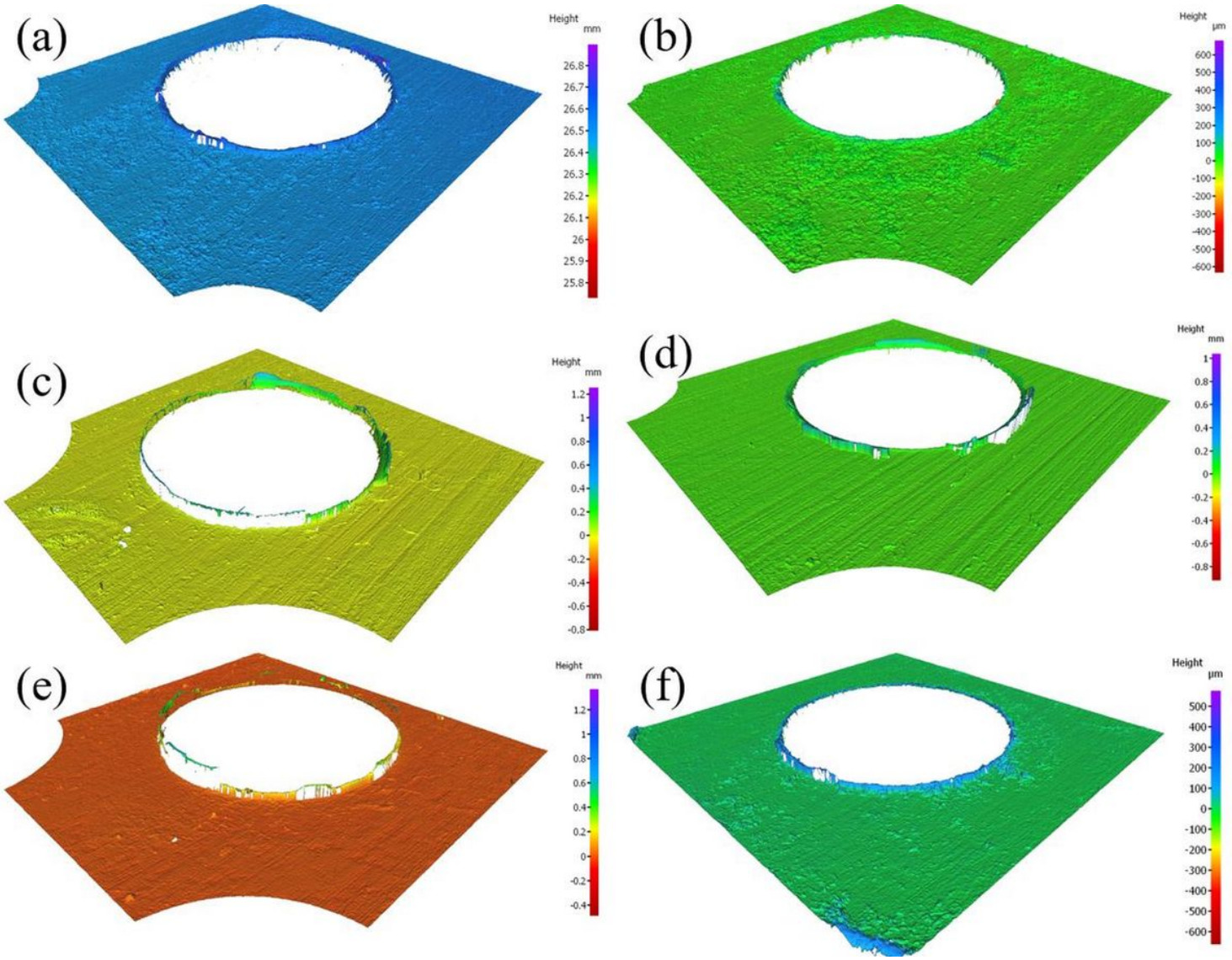

Figure 15

Effect of tool wear progression on the burr height at N= 3000 rpm for different machining parameters: (a) CD at first hole, (b) CD at hole number 50, (c) Am= 0.1mm at first hole, (d) Am= 0.1mm at hole number 50, (e) Am= 0.25mm at first hole, and (d) Am= 0.1mm at hole number 50, (e) Am= 0.25mm at first hole, and (d) Am= 0.25mm at hole number 50.

Coolant condition	**Dry**				**MQL**			
Amplitude (A_m)	**CD**	**0.1mm**	**0.16mm**	**0.25mm**	**CD**	**0.1 mm**	**0.16 mm**	**0.25 mm**
Flank wear land	≥ 300 µm	≤ 300 µm			≤ 300 µm			
Chisel edge	No fracture				No fracture	Fracture		
Exit delamination	Hole No≤ 20	Acceptable exit delamination factor			Acceptable exit delamination factor			
CFRP diameter accuracy	No	N/A		Yes	No	No		Yes
Ti diameter accuracy	No	N/A		Yes	Yes		Yes	

Figure 16

Effect of coolant condition on the CFRP/Ti6Al4V drilling process at N= 2000 rpm.